LEVEL Ⅱ ②

UNIAXIAL CYCLIC LOADING OF ELASTIC-VISCOPLASTIC MATERIALS

by

S. R. BODNER, I. PARTOM and Y. PARTOM

June 1978

78 09 13 120

REPORT DOCUMENTATION PAGE

1. REPORT NUMBER AFOSR-TR- 78-1298	2. GOVT ACCESSION NO.	3. RECIPIENT'S CATALOG NUMBER

4. TITLE (and Subtitle)	5. TYPE OF REPORT & PERIOD COVERED
UNIAXIAL CYCLIC LOADING OF ELASTIC-VISCOPLASTIC MATERIALS	INTERIM
	6. PERFORMING ORG. REPORT NUMBER MML Report No 61

7. AUTHOR(s)	8. CONTRACT OR GRANT NUMBER(s)
S. R. BODNER I. PARTOM Y. PARTOM	AFOSR-74-2607

9. PERFORMING ORGANIZATION NAME AND ADDRESS	10. PROGRAM ELEMENT, PROJECT, TASK AREA & WORK UNIT NUMBERS
TECHNION-ISRAEL INSTITUTE OF TECHNOLOGY MATERIAL MECHANICS LABORATORY HAIFA 32 000 ISRAEL	2307B2 61102F
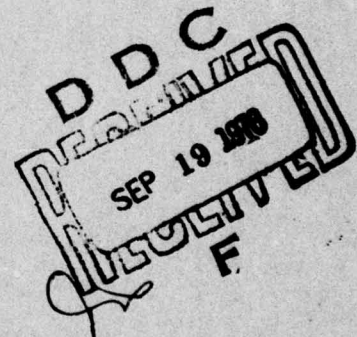
11. CONTROLLING OFFICE NAME AND ADDRESS	12. REPORT DATE
AIR FORCE OFFICE OF SCIENTIFIC RESEARCH/NA BLDG 410 BOLLING AIR FORCE BASE, D C 20332	June 1978
	13. NUMBER OF PAGES 31

14. MONITORING AGENCY NAME & ADDRESS(if different from Controlling Office)	15. SECURITY CLASS. (of this report)
	UNCLASSIFIED
	15a. DECLASSIFICATION/DOWNGRADING SCHEDULE

16. DISTRIBUTION STATEMENT (of this Report)

Approved for public release; distribution unlimited.

17. DISTRIBUTION STATEMENT (of the abstract entered in Block 20, if different from Report)

18. SUPPLEMENTARY NOTES

19. KEY WORDS (Continue on reverse side if necessary and identify by block number)

CYCLIC LOADING
VISCOPLASTICITY
FATIGUE
CONSTITUTIVE EQUATIONS
STRAIN RATE EFFECTS

BAUSCHINGER EFFECT

20. ABSTRACT (Continue on reverse side if necessary and identify by block number)

Elastic-viscoplastic constitutive equations based on two internal state variables are utilized to determine material response for uniaxial cyclic loading conditions. These equations are capable of representing the principal features of cyclic loading behavior including softening upon stress reversal, cyclic hardening or softening, tendency towards a stable limit cycle, cyclic relaxation, and cyclic creep. Calculations were performed for various stress and strain controlled conditions using material constants intended to represent commercially pure titanium and aluminum and OFHC copper. Capabilities and limitations of the analytical formulations are discussed in relation to computed results and corresponding test data.

DD $_{1\ JAN\ 73}^{FORM}$ 1473

UNIAXIAL CYCLIC LOADING OF
ELASTIC-VISCOPLASTIC MATERIALS

by

S.R. Bodner[1], I. Partom[2], Y. Partom[3]

ABSTRACT

Elastic-viscoplastic constitutive equations based on two internal state variables are utilized to determine material response for uniaxial cyclic loading conditions. These equations are capable of representing the principal features of cyclic loading behavior including softening upon stress reversal, cyclic hardening or softening, tendency towards a stable limit cycle, cyclic relaxation, and cyclic creep. Calculations were performed for various stress and strain controlled conditions using material constants intended to represent commercially pure titanium and aluminum and OFHC copper. Capabilities and limitations of the analytical formulations are discussed in relation to computed results and corresponding test data.

---

[1] Professor

[2] Research Engineer

[3] Adjunct Associate Professor

INTRODUCTION

Plastic deformation of an initially isotropic polycrystalline metal develops isotropic and directional anisotropic (i.e. stress sign dependent) changes. Analytical representations of these effects have concentrated on general multiaxial hardening laws with the classical isotropic and kinematic hardening models being special cases. The capabilities of some of these formulations have been discussed in the proceedings of recent conferences edited by Krempl [1], Saczalski and Stricklin [2], and Nemat-Nasser [3]. Comparisons are generally made to uniaxial cycling results which provide exacting tests of a theoretical model and are also technologically important.

Most of the proposed formulations consider directional anisotropic and isotropic hardening effects as completely separable and thereby controlled by different internal state variables and associated evolutionary equations, e.g., Rice [4], Kreig [5], Miller [6]. The directional anisotropic hardening component is usually represented by a "rest stress" or "back stress" which is intended as a stress tensor manifestation of microscopic residual stresses, and acts as an internal stress in resisting plastic deformation. Subtracting this stress from the applied stress leads to an "effective stress" which is taken to control plastic flow. In the basic kinematic hardening model, the "back stress" is the origin of the translated yield surface.

An alternative approach is to introduce internal state variables directly into the equation for plastic strain rate which

characterize the resistance of the material to plastic flow. This approach seems to be particularly suitable for plasticity theories that do not require a prescribed yield criterion, e.g. Bodner and Partom [7,8] and Hart [9]. For isotropic hardening conditions, the constitutive equations of Bodner and Partom utilized a single scalar inelastic state variable, referred to as the "hardness", which was a function of plastic work and which saturated at large plastic strains. These equations were shown to adequately represent material response for steady and varying strain rates, loading and unloading, stress relaxation, and creep (with a recovery term added) under uniaxial stresses of constant sign [8,10].

The present paper is concerned with extending the "hardness" concept to the case of uniaxial cyclic loading using the elastic-viscoplastic constitutive equations of Bodner and Partom. This requires introduction of a second hardness parameter to account for the directional character of resistance to plastic flow following deformation. An alternative approach based on a single, discontinuous inelastic state variable was used in an earlier study of this problem [11]; the present method is considered more basic and capable of generalization. Rules for determining the changes of the hardness parameters with loading history are developed in the paper. The equations are then applied to the cyclic loading of commercially pure titanium and aluminum and OFHC copper. Calculations were performed for strain controlled cycling of these metals and compared to corresponding test data. In addition, computations were made for conditions of cyclic creep and cyclic relaxation.

Although the work in this paper is based on two inelastic state variables, it is not presumed that these are sufficient for all aspects of cyclic loading which include a wide range of phenomena as described, e.g. by Morrow [12] and Jhansale [13]. The number and mathematical form of inelastic state variables required for different loading conditions for various materials has been discussed recently by Onat [14]. He indicates that constitutive equations based on two inelastic variables should be able to provide the main features of cyclic loading for certain classes of metals. Generalization of the inelastic state variable approach to the multi-dimensional stress case appears to be a difficult problem but some tentative suggestions have been made in [15]. This will be the subject of another paper.

FORMULATION OF CONSTITUTIVE EQUATIONS

AND HARDENING LAW

The basis of the elastic-viscoplastic constitutive equations developed by Bodner and Partom [7,8,16,17] is the separation of the total deformation rate d_{ij} into elastic (reversible) and plastic (non-reversible) components, d_{ij}^e and d_{ij}^p, which are taken to be always non-zero and functions of current values of state variables. Deformation rate is defined as the symmetrical part of the particle velocity gradient and would be equivalent to strain rate for small strains. Expressed mathematically, for the small strain case (present paper),

$$d_{ij} = d_{ij}^e + d_{ij}^p = \dot{\varepsilon}_{ij}^e + \dot{\varepsilon}_{ij}^p \tag{1}$$

For large strains, a strain measure is introduced into the analysis and the reference geometry is continually updated with deformation history, [7]. The elastic deformation rate is a function of stress rate through the time derivative of Hooke's Law for small strains and through a strain measure and strain energy functions for large strains.

The law governing plastic, i.e. non-reversible, deformations is taken to have the form of the Prandtl-Reuss flow law

$$d_{ij}^p = \underline{d}_{ij}^p = \lambda s_{ij} \tag{2}$$

where the bar symbol indicates the deviatoric component. Squaring eq. (2) leads to

$$D_2^p = \lambda^2 J_2 \qquad (3)$$

where D_2^p is the second invariant of the plastic deformation rate and J_2 is the second invariant of the stress deviator. A basic assumption of the formulation is that all non-reversible deformations are controlled by the relation

$$D_2^p = F_1(J_2, T, Z_k) \qquad (4)$$

where T is the temperature and Z_k are internal state variables whose current values contain all pertinent effects of prior inelastic deformations. On the basis of eqs. (3) and (4), d_{ij}^p in eq. (2) can be expressed as a function of stress, T, and the Z_k quantities.

To account for energy losses for reversible deformations and certain types of transient effects, an anelastic stress term σ_{ij}^a, which is not a state variable, could be added to the "elastic" stress σ_{ij}. It would represent an additional rate dependent resistance to flow of the material and could be significant for studies of internal damping [18] or for transient effects at high temperatures. At moderate temperatures, σ_{ij}^a is not a significant factor in plastic flow problems although it may influence the cyclic hysteresis curves of annealed metals. Another

transient effect that arises in cases of stress reversals is an apparent increased dislocation mobility acting over a short strain range. This can be accomodated by an additional term in eq. (2).

A particular form adopted in previous studies for eq. (4), for a constant temperature, is

$$D_2^p = D_0 \exp[-(Z^2/3J_2)^n (\frac{n+1}{n})]$$
(5)

which utilizes only a single internal variable Z. For conditions of isotropic hardening, Z was taken to be a scalar positive and increasing function of plastic work, $Z = f(W_p)$. Creep conditions would generally require addition of a hardness recovery (annealing) equation of the form

$$\dot{Z} = F_2(Z, J_2, T)$$
(6)

When σ_x is the only non-zero stress component, eqs. (2), (3) and (5) reduce to

$$d_x^p = \lambda s_x = \frac{2D_0}{\sqrt{3}} \frac{\sigma_x}{|\sigma_x|} \exp[-(1/2)(Z^2/\sigma_x^2)^n (\frac{n+1}{n})]$$
(7)

where d_x^p and s_x are the plastic deformation (strain) rate and the deviatoric stress in the axial (x) direction. Under cyclic loading, the material develops a directional characteristic with respect to resistance to plastic flow. In terms of inelastic state variables, there would therefore be a separate hardness value for each sign of the stress with the applicable quantity

used in eq. (7). There would be no actual discontinuity in plastic strain rate since $d_x^p = 0$ when the stress changes sign. The proposed rules for determining the changes in the hardness variables are as follows:

a. A single valued, positive, functional relation is taken to exist between the reference hardness parameter Z and plastic work W_p for a given material at a constant temperature T, i.e., $Z = f(W_p)$; this relation has a saturation value: $Z \rightarrow Z_1$ as $W_p \rightarrow \infty$.

b. Current values of the two hardness variables, Z_+, Z_-, corresponding to each sign of the stress, could be represented by points on the $f(W_p)$ curve where the associated W_p coordinates are taken as reference and not as absolute values.

c. An increment of loading to a new current stress σ_x leads to an increment of plastic work ΔW_p and an increment ΔZ given by

$$\Delta Z = f(W_p^0 + \Delta W_p) - f(W_p^0) \tag{8}$$

where W_p^0 is the W_p coordinate for the previous hardness state.

d. The corresponding changes in the two hardness variables to the loading increment are given by

$$(\Delta Z)_{+,-} = q(\Delta Z) \pm (1-q)(\Delta Z) \tag{9}$$

where q is a constant, $q \leqslant 1$; the positive sign in eq. (9) applies to the hardness variable in the current stress direction and the negative sign to that in the reverse direction; these increments are added to (or subtracted from) the previous values

at each load increment to give current values of the hardness variables which are always positive.

e. A change in sign of the stress requires application of the corresponding hardness variable in eq. (7).

Eq. (9) states that part of the hardness increment due to an increment in plastic work is isotropic (q) and the remainder (1-q), is directional. The total hardness increment in the direction of the current stress (assumed +), from eq. (9), would be

$$(\Delta Z)_+ = (\Delta Z) \tag{10}$$

and the decrement in the opposite direction

$$(\Delta Z)_- = -(1-2q)(\Delta Z) \tag{11}$$

Taking q = 1 corresponds to isotropic hardening and q = 0 could be interpreted as a form of kinematic hardening within a context of isotropic hardening since $Z = f(W_p)$. The parameter q enables representation of either cyclic hardening of softening with the former corresponding to $q > 0$ and the latter to $q < 0$. It is noted that a small excursion of stress reversal would have a negligible effect on the hardness variables if the plastic work for that excursion is small.

EXAMPLES

Among the experimental observations for cyclic loading are softening upon stress reversal, existence of a stable limiting stress-strain curve consequent to cyclic hardening or softening, and strain rate dependent effects such as cyclic creep and cyclic relaxation under appropriate loading conditions. To examine the capability of the proposed equations to represent these effects, a number of numerical exercises were performed for uniaxial cyclic loading of titanium, aluminum and copper. Titanium in the commercially pure condition has relatively high strain rate sensitivity and low work hardening. It was used as the reference material in earlier studies on uniaxial stress histories of constant sign [8]. The functional form used for $Z = f(W_p)$ for titanium was

$$Z = Z_1 - (Z_1 - Z_0) \exp(-m'W_p) \tag{12}$$

where Z_0, in this case, is a parameter defining $f(W_p)$ and the initial state point on the curve, $Z_i = Z_0$. In general, it is necessary to distinguish between Z_0 as a constant defining the $Z(W_p)$ curve and Z_i as the initial state point on that curve. Values of the material constants in eqs. (7) and (12) could be obtained from two monotonic stress-strain curves at different steady strain rates. The set of values obtained is not completely unique and a limited range of variations would result from different criteria of curve matching. For cyclic loading, the additional constant q, eq. (9), must be specified and this is chosen to pro-

vide for the observed degree of cyclic hardening or softening. In addition to these constants, the relevant elastic constant E or G must be specified.

Commercially pure aluminum and OFHC copper are relatively strain rate insensitive and experience large work hardening. To obtain more exact matching of the monotonic stress-strain curves for these materials, the m' factor in eq. (12) was generalized to the form

$$m' = m_0 + m_1 \exp(-\alpha W_p) \tag{13}$$

which introduces two more constants. The numerical exercises for Al and Cu reported here utilized eq. (13), but it is uncertain whether this refinement is fully necessary within the overall capabilities of the equations.

Values obtained for the material constants in eqs. (7) and (12) and the elastic constants for the reference metals are listed in Table 1. An additional material constant, C_1, is indicated in the list. It is introduced since changes of the hardness parameter alone would not lead to the softening observed immediately upon stress reversal. A tentative explanation of this effect on the microscopic level is that dislocations that were immobilized during the previous stress cycle become mobile over short ranges in the reverse direction. Such softening is therefore transient as the effect diminishes with increasing straining in the reverse direction. A method of providing for this effect is to add a term to d_{ij}^p, eq. (2), having either

of the forms

$$(d_{ij}^p)_{add} = C_1 [(Z^{max} - Z^{current})/(Z_0)^2] s_{ij} \tag{14a}$$

or

$$(d_{ij}^p)_{add} = C_2 [(J_2^{max} - J_2^{current})/(Z_0)^2] s_{ij} \tag{14b}$$

where Z^{max} and J_2^{max} are the maximum values of the parameters achieved in the previous cycle, and the total quantity in the brackets is taken to be positive or zero. These are essentially equivalent forms on the basis of eq. (4). The possible need to introduce eq. (14a) or (14b) indicates a limitation in using only two internal state variables in the formulation.

Calculations for uniaxial cyclic loading of the reference metals were performed based on the material constants obtained from steady rate stress-strain curves and suitable q's (Table 1). All the constants were determined from experiments at room temperature. Results are discussed for each metal separately.

a. Titanium (commercially pure):

These specimens were similar but not identical to those used in the tests reported in [8]. The constants are the same as those given in [8] with the difference that Z_0 is slightly lower and m' (=m/Z_0 of [8]) is somewhat higher. Experimental strain controlled stress-strain curves for ±1% strain in tension and compression are shown in Fig. 1. This material shows a small

amount of cyclic hardening and the associated parameter q was set
to be 0.05. Calculated stress-strain curves for a strain range
of ±1% are shown in Fig. 2. These results look reasonable except
for the sharp knee in the computed curves upon stress reversal
instead of the gradual curve of the test data. When eq. (14a)
is added to d_{ij}^p with $C_1 = 4\times10^{-2}\sec^{-1}$, then somewhat more realistic
curves, Fig. 3, are obtained. Numerical exercises with larger C_1's
and increased strain amplitudes showed local concavities in the
first few stress-strain cycles. Fig. 4 is an example of such
calculations for a strain range of ±2% using the same material
constants but with $C_1 = 5\times10^{-2}\sec^{-1}$. At strains of ±1% the
concavities commence when C_1 exceeds $7.5\times10^{-2}\sec^{-1}$. It is noted
that such effects have been observed experimentally [19] and have
been discussed by Asaro [20].

Under cyclic hardening conditions, $q > 0$, the maximum stress
increases with each cycle until a stable limit cycle is reached
with the stress level determined by the saturation value of Z, Z_1,
and the strain rate. For Z_1 constant, the stress will reach the
same maximum value for all cyclic strain amplitudes at the same
strain rate. This does not agree with experimental observations
which means that either Z_1, q, or some other parameter should be
treated as a third inelastic variable rather than as a simple con-
stant. Some preliminary numerical exercises taking Z_1 to vary
with cycling indicate more realistic limit cycles as well as better
agreement with other details. An alternative procedure that could
also lead to reasonable limit cycles is to let $q \to 0$ with cycling.

Some computations were also performed to demonstrate that cyclic softening does, in fact, occur when $q < 0$. Again, similar problems arise for the limit cycles which could be remedied by allowing Z_1 or q to vary with cycling.

Since the material characterization is time dependent, cyclic relaxation and cyclic creep should result from appropriate loading conditions. Strain controlled cycling between positive strain limits (1.25 and 0.225%) leads to cyclic relaxation, i.e. diminishing mean stress, as shown by the calculated curves in Fig. 5. Cycling between fixed stress limits under stress control with a non-zero mean stress leads to cyclic creep as shown in Fig. 6. The computations resulting in Figs. 5 and 6 did not include the added component to the plastic deformation rate, eq. (14a,b). They also did not include a hardness recovery term, eq. (6), which would have emphasized the relaxation and creep effects. Corresponding experimental data for these cases was not available, but the calculated results are similar to test results reported in the literature, e.g. [21,22,23].

b. Copper (OFHC, annealed):

Copper in its almost pure form shows some variation of mechanical properties for changes of impurity content and heat treatment. Nevertheless, it is frequently used for basic studies on material testing. Most of the material constants listed in Table 1 for copper were obtained in a previous study [10] and were based on experiments reported in [24]. The more elaborate expressions for $Z = f(W_p)$, eqs. (12) and (13), were used in this example. The

initial value of Z, Z_i, for copper is relatively small compared to the saturation value Z_1 which is an indication of relatively large work hardening. Copper is also relatively strain rate insensitive with a high n value (n = 9.2)

The cyclic hardening parameter q should be large enough to ensure that both Z parameters (i.e. in tension and compression) remain positive under cyclic loading. A minimum value for q is therefore inferred from eq. (11),

$$Z_{min} = Z_i - (1-2q)(\Delta Z)_{max} \geqslant 0 \qquad\qquad (15)$$

where $(\Delta Z)_{max} = Z_1 - Z_i$.

For copper, eq. (15) requires q to be equal to or greater than 0.425 for the viscoplastic constants listed in Table 1. A higher value, q = 0.55, was used in the calculations to match the strong cyclic hardening effects indicated in the reference experimental data for annealed OFHC copper [25].

Calculated stress-strain curves for strain controlled cycling of copper between ±1% strain are shown in Fig. 7 for $\dot{\epsilon} = 2 \times 10^{-4} sec^{-1}$. The additional plastic deformation term, eqs. (14a,b) seemed to be unnecessary in this case and was not used. Indicated in Fig. 7 are data points obtained from tests on annealed copper reported in [25] for almost exactly the same strain rate but over a narrower strain range. These seem to be in fairly good agreement with the

calculated results considering possible variations in specimen properties.

As in the case of titanium, the stable hysteresis loop will be determined by the saturation value of Z_1 and the strain rate, and would be the same for all strain amplitudes. A non-flat locus of stable hysteresis loops is actually observed for copper [12] which indicates again that introduction of another inelastic state variable is desirable for better overall matching.

c. 1100 Aluminum (commercially pure, annealed):

Commercially pure aluminum is also a standard reference material for mechanical testing although it exhibits variations of plastic response for differences in the type and amount of impurities and in the heat treatment. The viscoplastic material constants for aluminum listed in Table 1 (except for q) were based upon the steady rate stress-strain curves of [26]. Details of the impurity content and heat treatment of the specimens are also given in [26].

Although considerable work on cycling of 1100 aluminum was performed in the early 1960's, especially by L. F. Coffin and his associates, detailed stress-strain curves don't seem to be readily available. The cyclic hardening parameter q used for the calculations was therefore chosen by the criterion of eq. (15) and was 0.40 for the given viscoplastic constants. As a consequence, cyclic hardening will be fairly strong which is shown by the computed stress-strain curves in Fig. 8 for a strain controlled

amplitude of ±2%. Also indicated on Fig. 8 is an experimental 10th cycle stress-strain curve obtained from [23].

A comparison of results could only be in very general terms since the impurity contents and heat treatments of the specimens in [23] and [26] were not the same. In addition, the applied strain rate in [23] was not specified and may have been about a decade less than that used in the computations. The general shape and level of the indicated experimental stress-strain curve is, nevertheless, fairly close to the calculated curves for the third and fourth cycles. The overall agreement could probably be better with more exact correspondence of the material constants to the specimens used in the cyclic loading tests.

Aluminum also shows some degree of rate sensitivity; more than copper and less than titanium. The relevant material parameter in the equations is n which varies inversely with strain rate sensitivity. This parameter is 5 for Al compared to 1 for Ti and 9.2 for Cu. Aluminum would therefore experience cyclic creep and relaxation under appropriate loading conditions as reported in [23]. Calculated results for these cases would be similar to Figs. 5 and 6 but with greater cyclic hardening effects.

CONCLUSIONS

The main features of material response to uniaxial cyclic loading can be represented by the numerical integration of a set of incremental constitutive equations for the prescribed control conditions. These equations contain both elastic and visco-plastic components and utilize two inelastic variables in this application. Among the properties indicated by the computational results are softening upon stress reversal, cyclic hardening (or cyclic softening), a (strain rate dependent) asymptotic stable hysteresis loop, cyclic relaxation, and cyclic creep. The equations are capable, in principle, of treating arbitrary combinations of cyclic and monotonic loading.

An apparent limitation of the formulation is that the computed cyclic stress-strain curve, i.e. the locus of maximum stresses of the stable hysteresis loops, would be independent of the strain amplitude range and therefore flat. More realistic matching of this property could be obtained by treating the saturation value of the hardness parameter as a third, history dependent, inelastic state variable.

REFERENCES

1. Krempl, E. (editor), Proc. Conf. on "Inelastic Constitutive Equations for Metals - Experimentation - Computation - Representation," Rensselaer Poly. Inst., July 1974.

2. Saczalski, K.J. and Stricklin, J.A. (editors), Proc. of "Office of Naval Research Plasticity Workshop," Texas A & M Univ., Report 75-51, June 1975.

3. Nemat-Nasser, S. (editor), Proc. of "Workshop on Applied Thermoviscoplasticity," Technological Inst., Northwestern Univ., October 1975.

4. Rice, J.R., "Continuum Mechanics and Thermodynamics of Plasticity in Relation to Microscale Deformation Mechanisms," Chapter 2 in Constitutive Equations in Plasticity, A.S. Argon (ed.), MIT Press, Cambridge, Mass., 1975.

5. Krieg, R.D., "A Practical Two Surface Plasticity Theory," J. Applied Mechanics, vol. 42, 1975, pp. 641- .

6. Miller, A., "An Inelastic Constitutive Model for Monotonic, Cyclic, and Creep Deformation, Parts I and II," J. Engineering Materials and Tech., Trans. ASME, vol. 98, 1976, pp. 97-105(I), pp. 106-113(II).

7. Bodner, S.R. and Partom, Y., "A Large Deformation Elastic-Viscoplastic Analysis of a Thick-Walled Spherical Shell," J. Applied Mechanics, vol. 39, 1972, pp. 751-757.

8. Bodner, S.R. and Partom, Y., "Constitutive Equations for Elastic-Viscoplastic Strain-Hardening Materials," J. Applied Mechanics, vol. 42, 1975, pp. 385-389.

9. Hart, E.W., "Constitutive Relations for the Nonelastic Deformation of Metals," J. of Engineering Materials and Tech., Trans. ASME, vol. 98, 1976, pp. 193-202.

10. Bodner, S.R. and Merzer, A., "Viscoplastic Constitutive Equations for Copper with Strain Rate History and Temperature Effects," J. of Engineering Materials and Tech., Trans. ASME, 1978.

11. Bodner, S.R. and Partom, Y., "Constitutive Equations for Cyclic Loading of Rate Dependent Materials," MML Report No. 51, Technion, Haifa, 1976.

12. Morrow, J.D., "Cyclic Plastic Strain Energy and Fatigue of Metals," Internal Friction, Damping, and Cyclic Plasticity, ASTM STP 378, 1965, pp. 45-87.

13. Jhansale, H.S., "A History Dependent Parameter for the Cyclic Stress-Strain Behavior of Metals," T.A.M. Report No. 383, Univ. Illinois, Urbana, March 1974.

14. Onat, E.T., "Representation of Inelastic Behavior," Report to ORNL, Dept. of Engin. and Applied Science, Yale Univ., Nov. 1976.

15. Bodner, S.R., "A Hardness Law for Inelastic Deformation," Letters in Applied and Engin. Sciences (Inter. J. of Engin. Science), vol. 16, 1978, pp. 221-230.

16. Partom, Y., "Numerical Solution of Continuum Mechanics Problems," D.Sc. Thesis, Technion, Haifa, 1967; (also, Report No. 11, Material Mechanics Laboratory, Technion, Haifa, September 1967).

17. Bodner, S.R., "Constitutive Equations for Dynamic Material Behavior," Proc. of Confer. on Mechanical Behavior of Materials Under Dynamic Loads, U.S. Lindholm (ed.), Springer-Verlag Pub., N.Y., 1968, pp. 176-190.

18. Derman, D., Zaphir, Z., and Bodner, S.R., "Nonlinear Anelastic Behavior of a Synthetic Rubber at Finite Strains," J. Rheology, vol. 22, 1978.

19. Stoltz, R.E. and Pelloux, R.M., "Cyclic Deformation and Bauschinger Effect in Al-Cu-Mg Alloys," Scripta Metallurgica, vol. 8, 1974, pp. 269-276.

20. Asaro, R.J., "Elastic-Plastic Memory and Kinematic-Type Hardening," Acta Metallurgica, vol. 23, 1975, pp. 1255-1265.

21. Landgraf, R.W., in *High Fatigue Resistance in Metals and Alloys*, ASTM STP 467, 1970, pp. 3-36.

22. Sandor, B.I., *Fundamentals of Cyclic Stress and Strain*, Univ. of Wisconsin Press, 1972.

23. Coffin, L.F., "The Influence of Mean Stress on the Mechanical Hysteresis Loop Shift of 1100 Aluminum," J. Basic Engin., Trans. ASME, vol. 86, series D., 1964, pp. 673-680.

24. Senseny, P.E., Duffy, J., and Hawley, R.H., "Experiments on Strain Rate History and Temperature Effects During the Plastic Deformation of Close-Packed Metals," J. Applied Mechanics, vol. 45, 1978, pp. 60-66.

25. Lamba, H.S. and Sidebottom, O.M., "Biaxial Cyclic Hardening of Annealed Copper Cylinders Evaluated by Deformation Plasticity Theories," T.A.M. Report No. 406, University of Illinois, Urbana, January 1976.

26. Lindholm. U.S., Yeakley, L.M., and Bessey, R.L., "An Investigation of the Behavior of Materials Under High Rates of Deformation," Report AFML-TR-68-194, Air Force Materials Lab., WPAFB, Ohio, July 1968.

LIST OF CAPTIONS

Fig. 1 - Experimental stress-strain curves for titanium subjected to ten cycles of ±1% strain (tension/compression).

Fig. 2 - Computed stress-strain curves for titanium for ±1% strain (tension/compression) using material constants of Table 1 with $C_1 = 0$.

Fig. 3 - Computed stress-strain curves for titanium for ±1% strain (tension/compression) using material constants of Table 1 ($C_1 = 4 \times 10^{-2} \sec^{-1}$).

Fig. 4 - Computed stress-strain curves for titanium for ±2% strain (tension/compression) showing local concavities; material constants of Table 1 with $C_1 = 5 \times 10^{-2} \sec^{-1}$.

Fig. 5 - Computed stress-strain curves for titanium for strain controlled cycling with positive strain limits showing creep relaxation.

Fig. 6 - Computed stress-strain curves for titanium for stress controlled cycling with a positive mean stress showing cyclic creep.

Fig. 7 - Computed and experimental stress-strain curves for annealed OFHC copper under strain controlled cycling (tension/compression); computations based on constants of Table 1.

Fig. 8 - Computed and experimental stress-strain curves for annealed 1100 aluminum for ±2% strain (tension/compression); computations based on constants of Table 1.

Table 1

Material Constants

a. Elastic Constants:

	Ti	Cu	Al
E(MPa)	12.0×10^4	12.0×10^4	6.8×10^4

b. Viscoplastic Constants, eqs. (5), (9), (12), (13), (14a):

	Ti	Cu	Al
$D_0 (\text{sec}^{-1})$	10^4	10^4	10^4
n	1	9.2	5
$Z_0 (=Z_i)(\text{MPa})$	1000	31	25
$Z_1 (\text{MPa})$	1400	237	150
$m'(\text{MPa})^{-1}$	0.35	–	–
$m_0 (\text{MPa})^{-1}$	–	0.15	0.15
$m_1 (\text{MPa})^{-1}$	–	0.25	0.45
$\alpha(\text{MPa})$	–	0.50	0.30
q	0.05	0.55	0.40
$C_1 (\text{sec})^{-1}$	4×10^{-2}	0	0

TITANIUM
experimental
$\dot{\epsilon} = 3.2 \times 10^{-3}$ sec^{-1}

FIG. 1

FIG. 2

FIG. 3

σ
(MPa)

200

100

0

-100

-200

-2.0   -1.5   -1.0   -0.5   0   0.5   1.0   1.5   2.0

ε (%)

④ ③   ② ①

① ② ③

TITANIUM
calculated
$C_1 = 5 \times 10^{-2} \, sec^{-1}$
$\dot{\epsilon} = 3.2 \times 10^{-3} \, sec^{-1}$
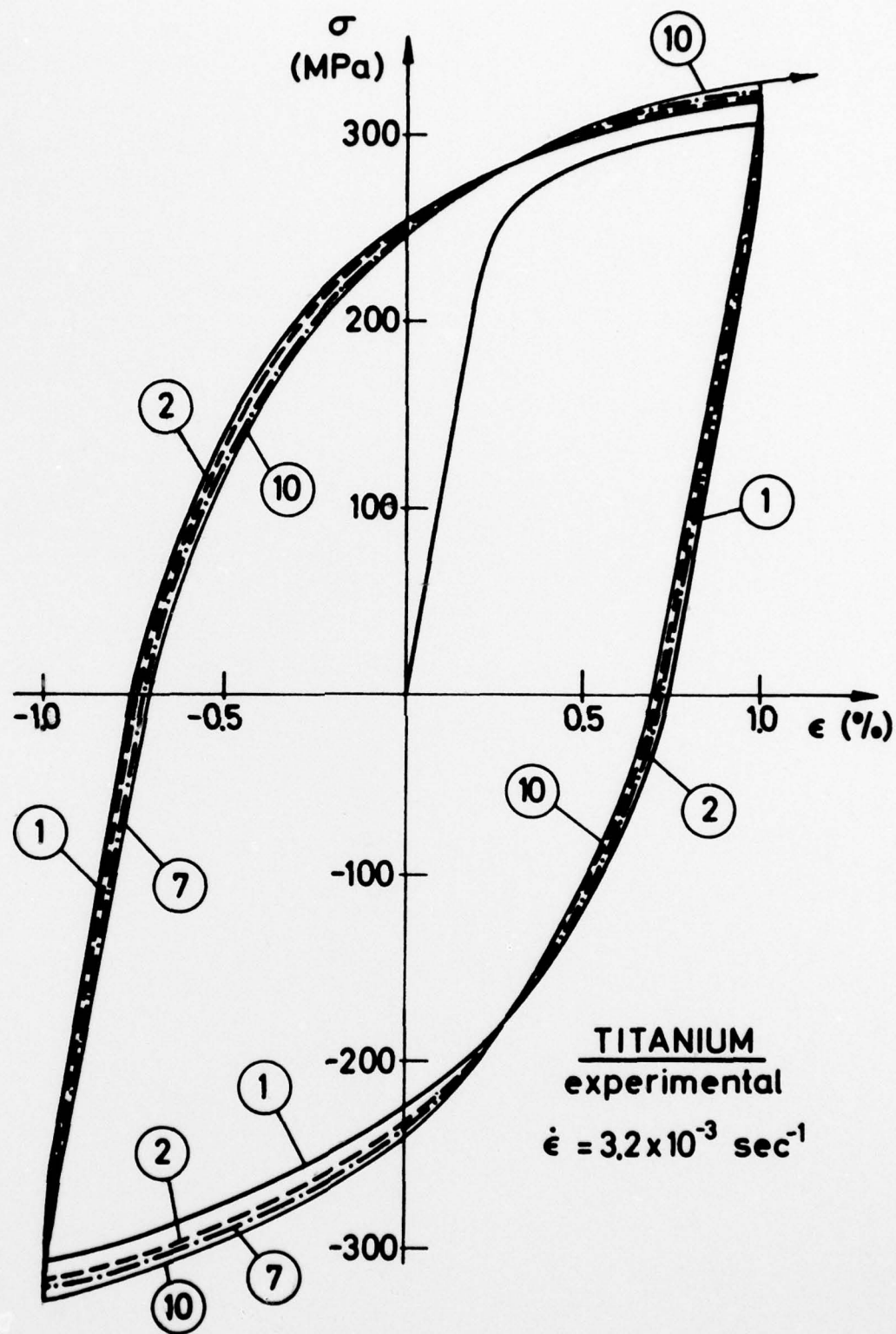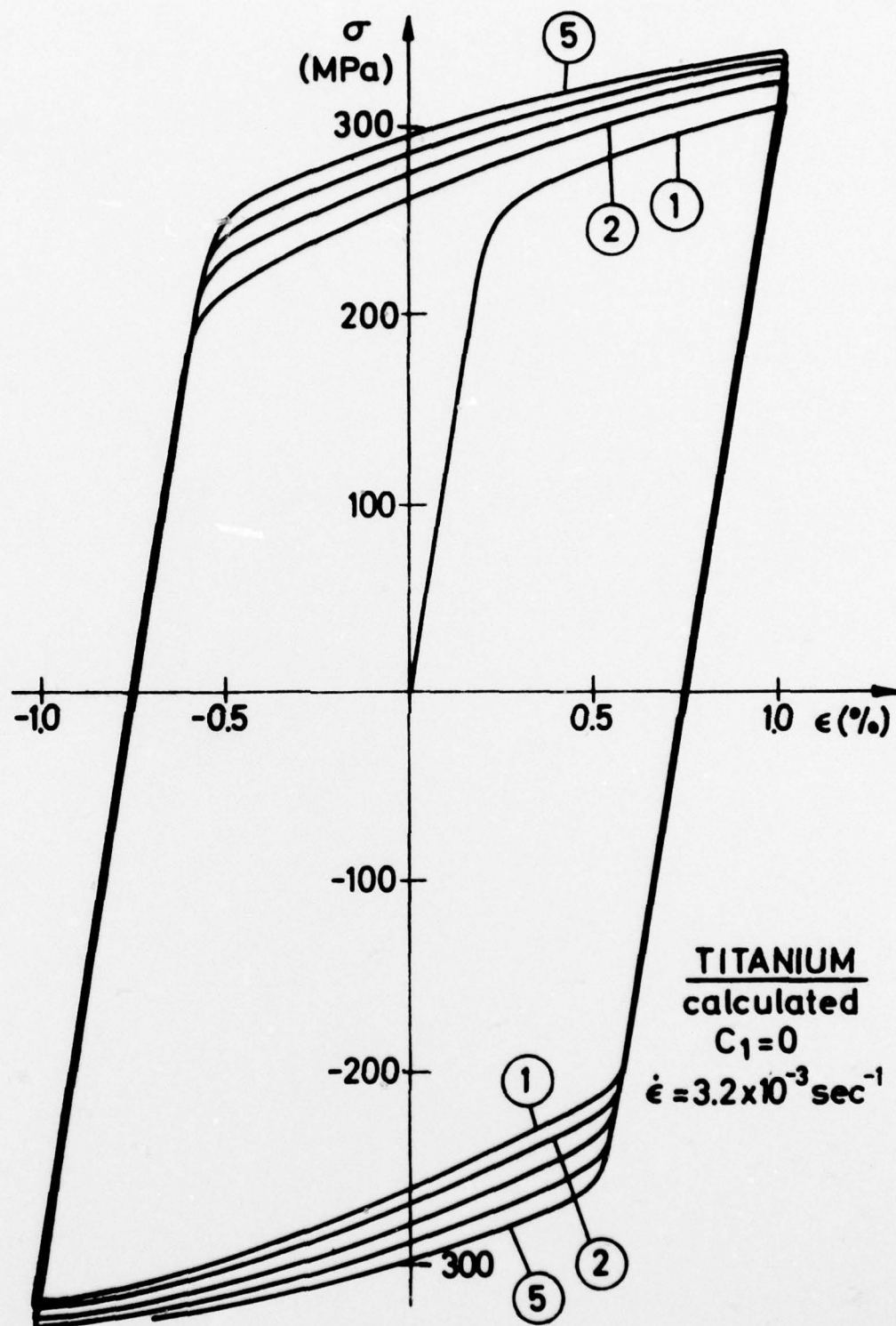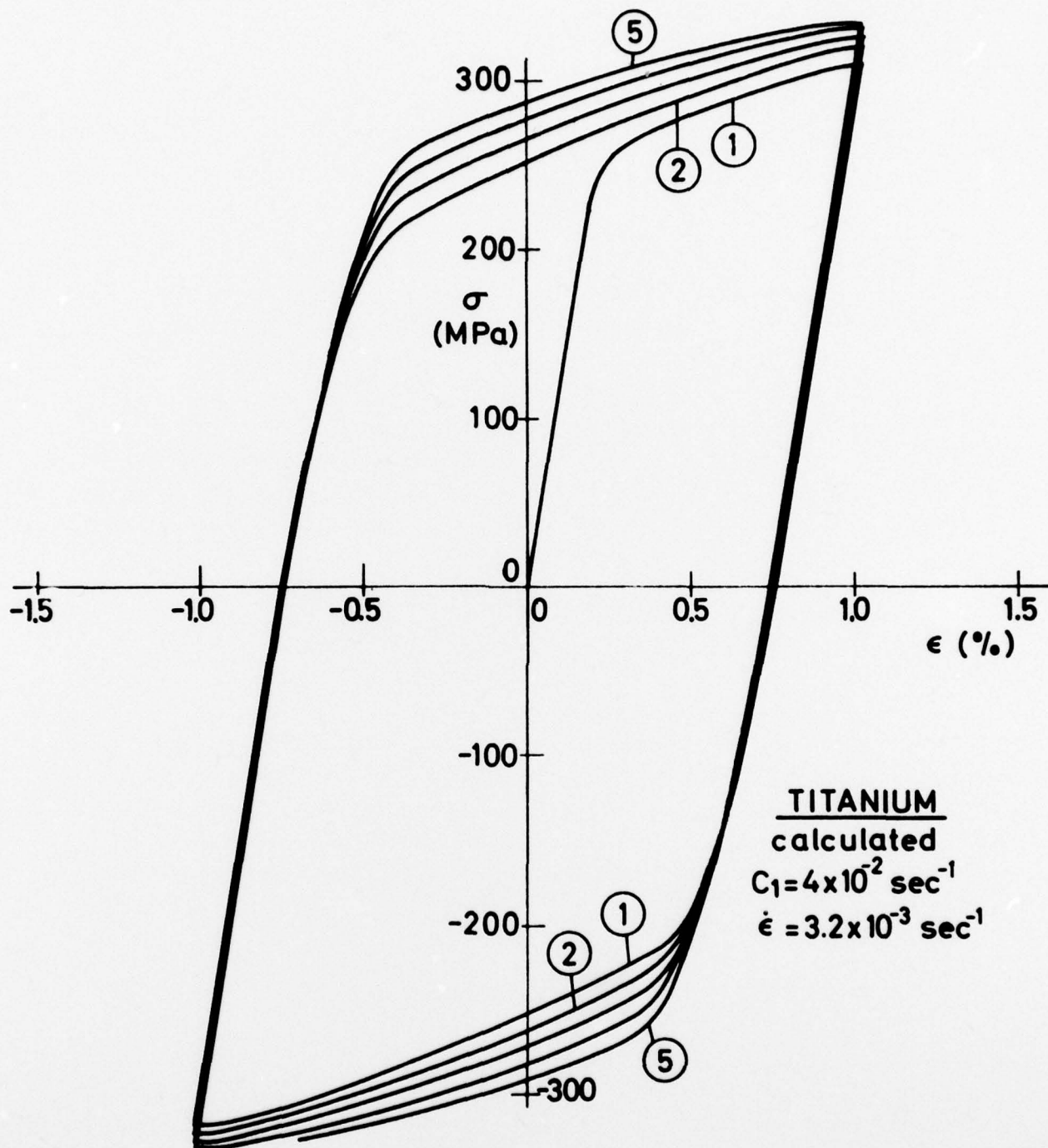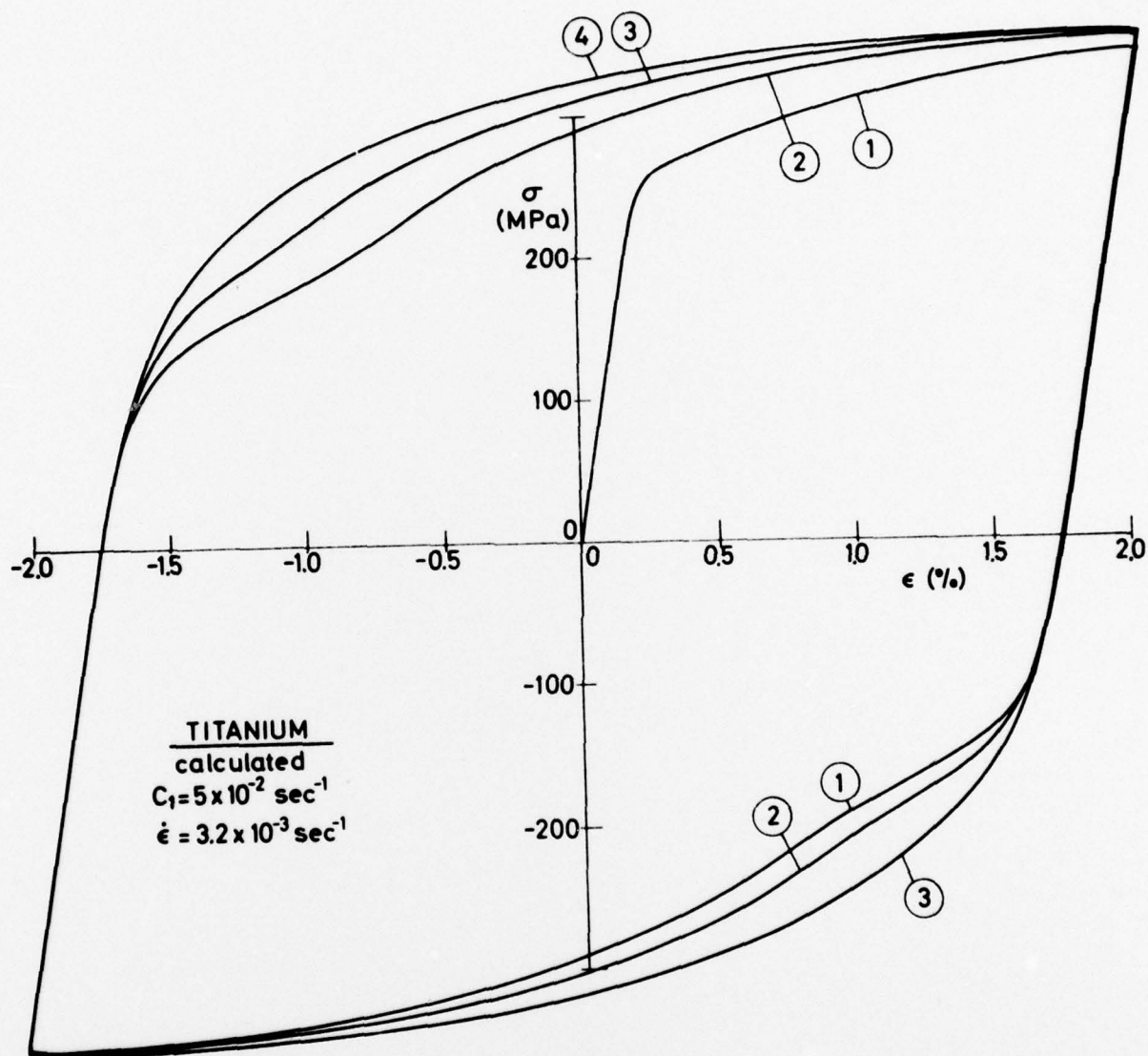
FIG. 4

TITANIUM
strain control
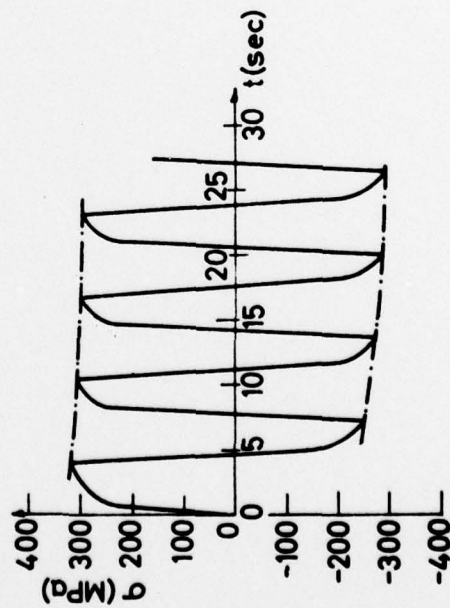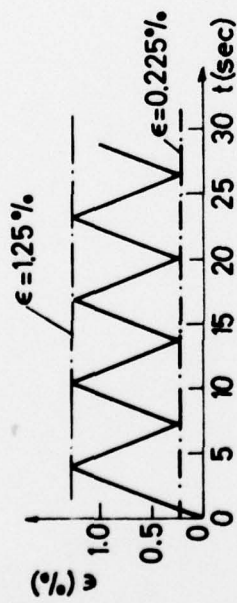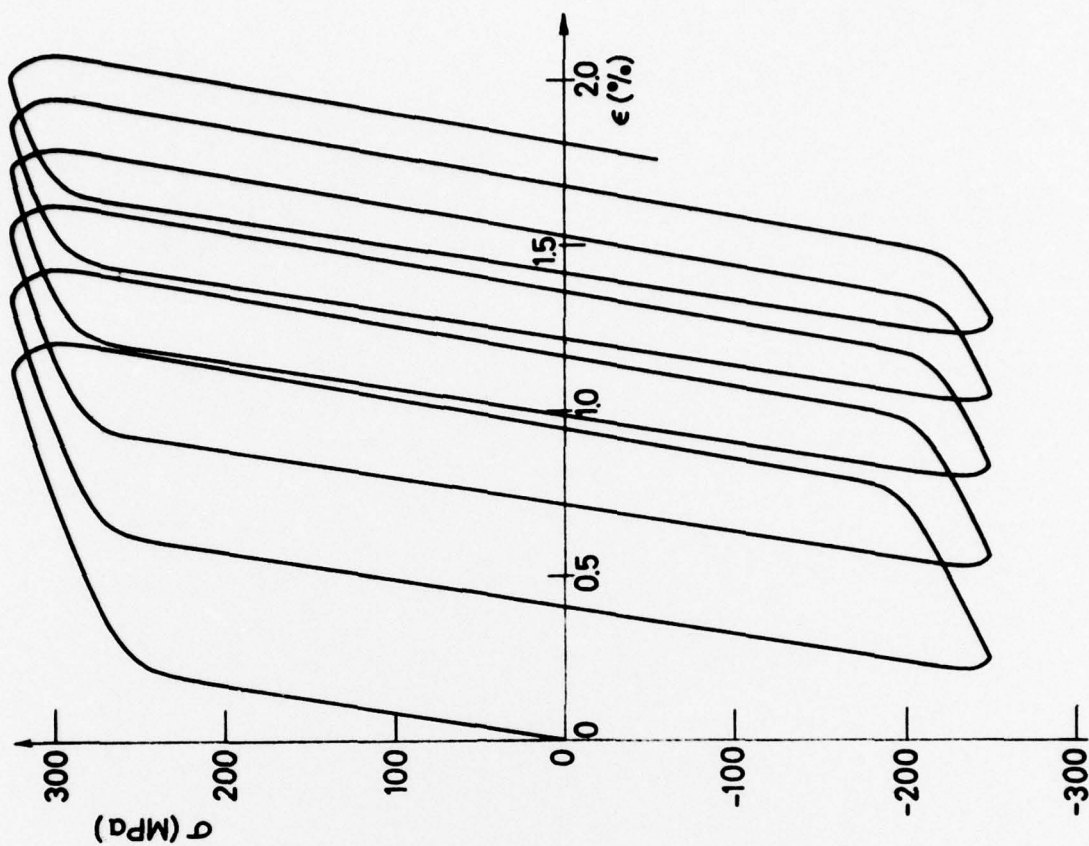$\dot{\epsilon} = 3.2 \times 10^{-3} \, \text{sec}^{-1}$

FIG. 5

TITANIUM
stress control

FIG. 6

FIG. 7

ALUMINUM, ± 2% ε
ε̇ = 2×10⁻³ sec⁻¹

F I G. 8